

# High efficiency regimes of ion acceleration

F. Pegoraro

WE-Heraeus-Seminar 2007

## Outline

- *The electric fields produced by the interaction of ultra-short and ultra-intense laser pulses with a thin target make it possible to obtain multi-MeV, high density, highly collimated proton and ion beams with extremely short duration, in the sub-picosecond range.*
- *Critical features are the efficiency of the ion acceleration process and the energy spectrum of the produced ion beam.*
- *At high laser intensities a very efficient acceleration regime has been predicted where the radiation pressure of the laser pulse plays a major role. Results on the stability of this regime will be presented in this talk after an introduction on laser acceleration.*

## Introduction

The effective ion acceleration during the interaction of an ultra short and ultra intense laser pulse with matter is possibly one of most important results in the investigation of the interaction of multi-terawatt and petawatt power laser pulses with plasmas.

● In the last six years collimated beams of fast protons have been produced where electron energies in the hundreds of  $MeV$  range were observed while the protons have a broad spectrum, with maximum energies up to a few tens of  $MeV$ <sup>1</sup>. Compared to conventional accelerators these proton beams have a very high brilliance and are very directional, with a divergence of a few degrees at the highest energies and an apparent source size of less than  $5 - 10 \mu m$ . The number of particles in the beams can approach  $10^{13}$  with good conversion efficiency of the laser energy into the energy of fast ions. The beams are emitted in bursts of  $ps$  duration, three orders of magnitude shorter than conventional accelerator bunches.

---

<sup>1</sup>A. Maksimchuck *et al.*, *Phys. Rev. Lett.*, **84** 4108 (2000); E.L. Clark *et al.*, *Phys. Rev. Lett.*, **85** 1654 (2000); S.P. Hatchett *et al.* *Phys. Plasmas*, **7** 2076 (2000); R.A. Snavely *et al.*, *Phys. Rev. Lett.*, **85** 2945 (2000); A.J. Mackinnon *et al.*, *Phys. Rev. Lett.*, **86** 1769 (2001); M. Hegelich *et al.*, *Phys. Rev. Lett.*, **89** 085002 (2002); M. Roth, *et al.*, *Phys. Rev. Special Topics*, **AB 5**, 061301 (2002); M. Zepf, *et al.*, *Phys. Rev. Lett.*, **90**, 064801 (2003); H. Schwöerter, *et al.*, *Nature*, **439**, 445 (2006); M. Hegelich, *et al.*, *Nature*, **439**, 441 (2006), S. Ter-Avetisyan, *et al.*, *Phys. Rev. Lett.*, **96**, 145006 (2006); A.V. Brantov, *et al.*, *Phys. Plasmas*, **13** 122705 (2006).

These laser-produced ion beams have important applications ranging from the fast ignition of thermonuclear targets, to proton imaging, deep proton lithography, medical physics, and injectors for conventional accelerators.

*Although the basic physical mechanisms of ion beam generation in the plasma produced by the laser pulse interaction with the target are common to all these applications, each application requires a specific optimization of the ion beam properties i.e., an appropriate choice of the target design and of the laser pulse intensity, shape and duration.*

*Indeed different ion acceleration regimes are encountered in the interaction of ultraintense laser pulses with a target<sup>2</sup>.*

---

<sup>2</sup>See e.g. S.V. Bulanov, *et al.*, *Plasma Phys. Reports*, 30, 196 (2004).

## Acceleration regimes and beam properties

When laser pulses with powers corresponding to relativistically strong fields are used, a transition occurs from an essentially quasineutral, lower intensity regime where the heated Boltzmann electrons accelerate the ions up to energies, per ion unit charge, of the order of the electron temperature<sup>3</sup> to a new regime where dynamical charge separation effects are dominant and a fraction of the ions can acquire an energy that is substantially larger than the electron thermal energy.

---

<sup>3</sup>see e.g. P. Mora, *Phys. Rev. Lett.* , **90**, 185002 (2003).; S. Betti, *et al.*, *Plasma Phys. Contr. Fus.*, **47**, 521 (2005); F. Cornolti, *et al.*, *Phys. Rev. E* 71, 056407-1 (2005); M. Passoni, *et al.*, *Phys. Rev. E* **69**, 026411 (2004); P. Mora, *Phys. Rev. E* , **72**, 056401, (2005)

Extensive investigations with multi-dimensional Particle In Cell simulations have confirmed that collimated beams of fast protons with energies in the several MeV range can be obtained by optimizing the laser-target parameters<sup>4</sup>.

---

<sup>4</sup> T. Esirkepov, *et al.*, *JETP Lett.* **70**, 82 (1999); S. Bulanov, *et al.*, *JETP Lett.* , **71**, 407 (2000); Y. Sentoku, *et al.*, *Phys. Rev.* , **E 62**, 7271 (2000); H. Ruhl, *et al.*, *Plasma Phys. Rep.* , **27**, 411 (2001); Y. Sentoku, *et al.*, *Appl. Phys.* , **B 74**, 207 (2002); T. Nakamura, *Phys. Rev.* , **E 67**, 026403, (2003); T. Esirkepov, *et al.*, *Phys. Rev. Lett.* , **89**, 175003 (2002); S. Bulanov, *et al.*, *Plasma Physics Reports*, , **28**, 975 (2002); A. Macchi, *et al.*, *Phys. Rev. Lett.* , **94**, 165003 (2005); L. Romagnani, *et al.*, *Phys. Rev. Lett.* , **95**, 195001 (2005); \* T. Esirkepov, *et al.*, *Phys. Rev. Lett.* , **96**, 105001 (2006); B. J. Albright, *et al.*, *Phys. Rev. Lett.* , **97**, 115002 (2006); L. Badziak, *et al.*, *Appl. Phys. Lett.* , **89**, 1504 (2006); A.P.L. Robinson, *et al.*, *Phys. Rev.* , **E 75**, 015401 (2007); .

## Digression on old 3D results

As an example, here we may recall some "old" numerical results of the 3-D simulations of the interaction of an ultrashort ultra intense laser pulse with a plasma slab<sup>5</sup>.

The aim of these simulations was to find the maximum energy that the ions can gain in the fields created by the **nonadiabatic** interaction on the laser pulse with a plasma slab.

Two acceleration phases were identified: a first phase when the ions propagate inside the partly evacuated channel along the pulse path and are accelerated by a relativistically propagating double layer structure, and a second phase where they are accelerated in vacuum after they exit the slab both electrostatically due to the expansion of the plasma electron cloud and electromagnetically due to the expansion of the self-generated magnetic field carried by the plasma.

---

<sup>5</sup>F. Pegoraro, *et al.*, IEEE Trans. Plasma Science, **28**, 1226, (2000).

A short ( $15\lambda$ ) plasma slab with  $\omega/\omega_p = 1$  was considered with  $\omega_p$  the nonrelativistic unperturbed plasma frequency and mass ratio corresponding to a hydrogen plasma.

The pulse was circularly polarized with amplitude  $a_e \simeq 50$ , slightly larger than the square root of the mass ratio, the pulse length is  $20\lambda$  and its width is  $10\lambda$ . In these 3-D run 8 particles per species, per cell were used (the total number per species was  $\sim 18.5$  millions).

The formation of the channel in the ion density in the 3-D plasma slab is shown in Fig.1 at  $t = 30$  projected on the horizontal  $x$ - $y$  plane at  $z = 0$ , frame (a), and on the transverse  $y$ - $z$  plane at  $x = 15\lambda$ , frame (b).

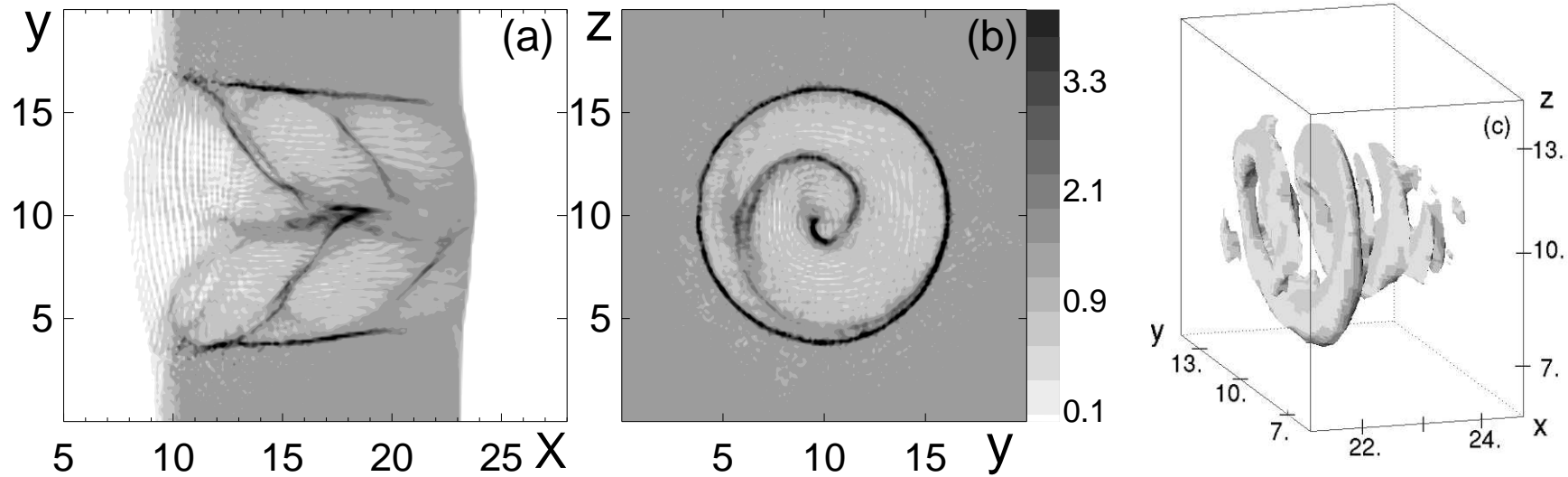


Figure 1: The  $x-y$  distribution at  $z = 0$  (a), the  $y-z$  distribution (b) of the ion density at  $x = 15\lambda$  and the isosurface  $\sqrt{(E^2 + B^2)/2} = 40$  of the electromagnetic energy density (c) in the case of the pulse propagating in the 3-D plasma slab.

The circularly polarized pulse has carved a staircase structure which resembles the helical chamber inside a shell.

A similar helix, although less sharp, is also seen in the electron density and in Fig.1c where the isosurface of the electromagnetic energy density corresponding to the amplitude value  $\sqrt{(E^2 + B^2)}/2 = 40$  is shown.

The expansion and acceleration of the ions in the vacuum region, following the electron expansion when the pulse has drilled a hole through the slab, is shown in Fig.2 at  $t = 48$ .

The  $x - y$  section at  $z = 0$  of the ion density distribution shows a strongly collimated beam along the  $x$  axis.

This beam collimation is also seen in the 3-D plot where the isosurface corresponding to  $n_i = 1.8$  is shown.

We see that the beam is strongly collimated.

The longitudinal ion momentum distribution at  $t = 48$  is shown in Fig.2c.

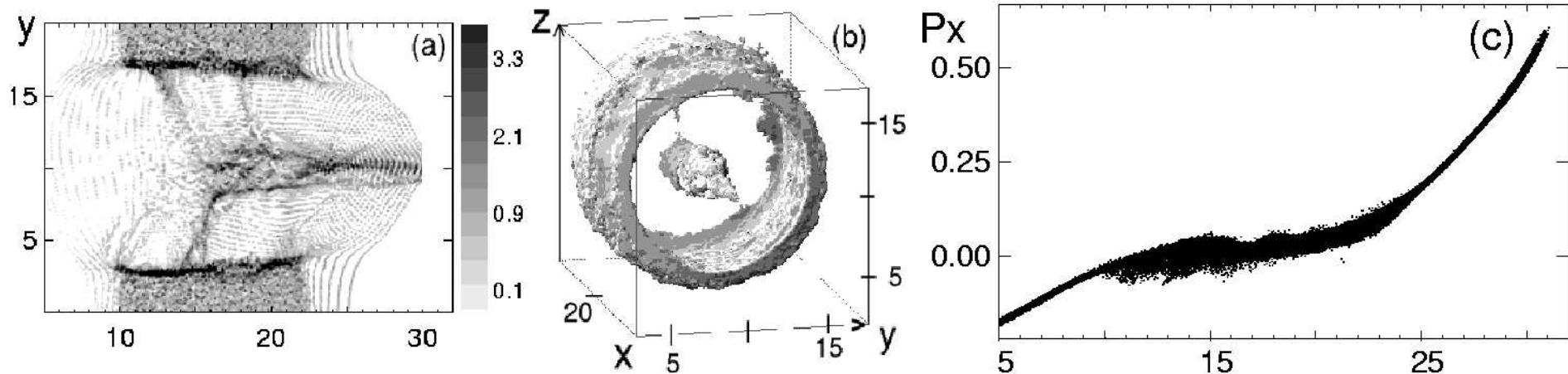


Figure 2: The  $x$ - $y$  distribution at  $z = 0$  (a), and the isosurface  $n_i = 1.8$  of the ion density (b) at  $t = 48$  ( $2\pi/\omega$ ), the ion phase space  $(P_x, x)$  (frame c) in the case of the pulse propagating in the 3-D plasma slab.

## Ion acceleration requirements

Besides the maximum energy reached, an important issue in the investigation of the different ion acceleration mechanisms, is the quality of the beam produced in terms of spatial collimation and in particular of energy resolution.

Proton beams with relatively wide energy spectrum do indeed provide a novel and effective diagnostic tool for detecting the electromagnetic fields generated by the laser pulse in the plasma<sup>6</sup> but, because of their broad 'thermal' energy spectra, such beams are not appropriate for applications where energy selection is an issue.

---

<sup>6</sup>see M. Borghesi, *et al.*, *Plasma Phys. Control. Fus.*, **43**, A267 (2001); M. Borghesi *et al.*, *Phys. Rev. Lett.*, **88**, 135002 (2002); M. Borghesi, *et al.*, *Phys Plasmas* **9**, 2214 (2002), M. Borghesi, *et al.*, *Phys Plasmas* **94**, 195003 (2005).

This is of particular importance when the use of laser accelerated proton beams is proposed in order to provide a controlled and localized delivery of energy, such as in the scheme of the proton driven fast ignition<sup>7</sup> of a thermonuclear pellet or in the applications to hadrontherapy in oncology<sup>8</sup>

---

<sup>7</sup>M. Roth, *et al.*, *Phys. Rev. Lett.* **86**, 436 (2001); S. Atzeni, *et al.*, *Nucl. Fusion* **42**, L1 (2002); M. Temporal, *et al.*, *Phys. Plasmas* **9**, 3098 (2002).

<sup>8</sup>V.Khoroshkov, *et al.*, *Eur. J. Phys* ; **19**, 523 (1998); G. Kraft, *Physica Medica XVII, Suppl.*; **1**, 13 (2001); U. Amaldi, *Physica Medica XVII, Suppl.* , **1**, 33 (2001); M. Goiten, *et al.*, *Phys. Today* ; **55**, 45 (2002); S. Bulanov *et al.*, *Plasma Phys. Rep.*; **28**, 453 (2002); S. Bulanov *et al.*, *Phys. Lett.*; **A 299**, 240 (2002).

## Digression on proton imaging

Proton imaging employs proton beams as a diagnostic tool in a point-projection imaging scheme and provides the possibility of identifying electric fields in dense plasmas and laser-irradiated targets with unprecedented spatial and temporal resolution<sup>9</sup>

The proton beams need not be monochromatic for this application, indeed a broad spectrum can be advantageous, as it allows multiframe capability.

The targets used for proton beam production are thin foils that act as the source of the proton beam. The electro-magnetic fields in a plasma between the source and the detector distort the geometrical propagation of the protons.

---

<sup>9</sup> M. Borghesi, *et al.*, Plasma Phys. Control. Fus. **43**, A267 (2001)

In this way electric fields, slowly varying on the proton crossing time, can be detected with micron spatial resolution and their evolution can be followed on a picosecond time scale.

This high temporal resolution makes laser produced proton beams ideal in order to detect coherent field structures arising from the nonlinear plasma dynamics following intense, short pulse interactions.

The potentialities of this method are apparent from the results shown in Fig.3 on the time evolution of the sheath electric field at the rear side of the target<sup>10</sup>.

---

<sup>10</sup>L. Romagnani, *et al.*, *Phys. Rev. Lett.*, **95**, 195001 (2005)

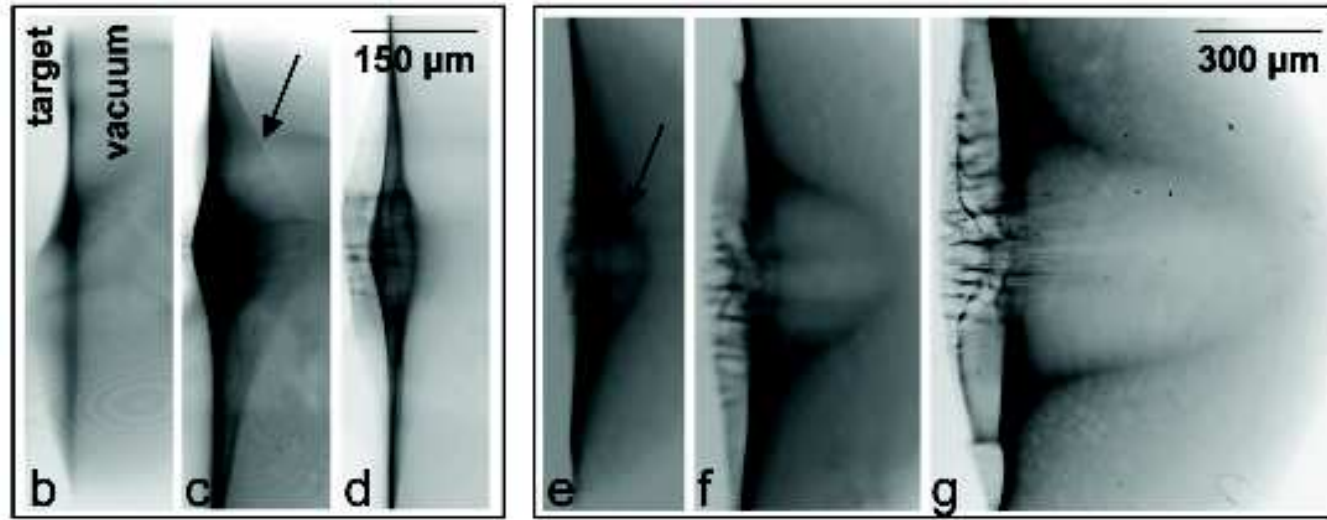


Figure 3: Proton imaging of accelerating sheath electric field at the rear side of the target.

## Oncological proton therapy and double layer targets

### Digression on proton therapy

The use of protons in radiotherapy for cancer treatment has several advantages:

- i) the proton beam scattering on the atomic electrons is weak and thus there is less irradiation of healthy tissues in the vicinity of the tumor,
- ii) the slowing down length for a proton with given energy is fixed, which avoids undesirable irradiation of healthy tissues at the rear side of the tumor,
- iii) the well localized maximum of the proton energy losses in matter (the Bragg peak) leads to a substantial increase of the irradiation dose in the vicinity of the proton stopping point.

However the construction and operation costs of hospital-based proton therapy centers remain comparatively higher than those of the most expensive conventional beam therapy plants designed for radiation therapy.

An attractive possibility of reducing such costs is to use ultrashort, ultraintense laser pulses to produce the proton beams. In this scheme the laser radiation is delivered to the target where its energy is converted into the energy of fast protons. In this approach the central accelerator, the channels through which the fast protons are transported and most of the gantry, which provides multi-directional irradiation of a laying patient, is no longer required.

The basic parameters required for a proton beam to be used for medical applications can easily be reached with present accelerator technology. The proton beam intensity must be in the  $10^{10}$  to  $5 \times 10^{10}$  protons per second range, the maximum proton energy must be in the 230 to 250 *MeV* range. For laser accelerators the most demanding conditions are the requirement for a highly monoenergetic proton beam with  $\Delta\mathcal{E}/\mathcal{E} = 10^{-2}$  and the system duty factor i.e., the fraction of the time during which the proton beam can be used which is important in determining the economical feasibility of the use of a laser accelerator.

## A possible method of achieving high quality proton beams

The main physical challenge is to devise a method of producing proton beams of sufficiently high quality in terms of energy resolution to ensure that a substantially high and homogeneous dose is delivered to the tumor while sparing neighboring healthy tissues.

The basic idea behind this proposal is to make the interaction between the laser pulse and the plasma strongly non adiabatic by using short laser pulses and a target made of a layer of heavy ions followed by a thin proton layer with a transverse size smaller than the pulse waist<sup>11</sup>.

Double layer targets were shown experimentally<sup>12</sup> to provide a considerable increase in energies and current of protons produced.

---

<sup>11</sup>S. Bulanov *et al.*, *Plasma Phys. Rep.*, **28**, 453 (2002); S. Bulanov *et al.*, *Phys. Lett.*, **A 299**, 240 (2002).

<sup>12</sup>J. Badziak, *et al.*, *Phys. Rev. Lett.*, **87**, 215001 (2001); J. Badziak, *et al.*, *J. Appl. Phys.*, **91**, 5504 (2002).

In this layered target scheme a foil is used as the target and its rear surface is coated with a thin and transversally narrow hydrogen layer,

More recently the effectiveness of this method seems to have been proved experimentally<sup>13</sup>

An ultrashort ultraintense laser pulse irradiates the target: the heavy atoms are partly ionized and most of the resulting free electrons abandon the foil. This leads to a large electric field due to charge separation.

Heavy ions with large mass to charge ratio remain at rest while the protons in the coating are accelerated. If the proton coating is thin and has a transverse size smaller than the diameter of the focal spot of the laser pulse, this scheme provides a controlled acceleration of protons.

---

<sup>13</sup>H. Schwoerer, *et al.*, *Nature*, **439**, 445 (2006),

The electrons escaping the heavy ion foil under the action of the ponderomotive pressure of the laser radiation give rise to a quasistatic electric field caused by the non-neutralized electric charge. This field is localized in a finite region with dimensions comparable to the transverse dimension of the laser pulse.

In this initial stage the protons are accelerated by this electric field before the heavy ions of the first layer start to move.

If the total number of protons is small in comparison with the number of electrons that have escaped from the target, the effect of the electric field of the protons on their dynamics can be neglected.

In this case the proton acceleration can be described in the approximation of test particles moving in an assigned electric field. The energy of these protons can approach  $2m_p c^2 a_0^2$  where  $a_0 = eE_0/m_e c \omega_0$  is the dimensionless amplitude of the laser pulse,  $m_p$  is the proton mass and the energy of the electrons in the cloud has been estimated to be of the order of  $a_0 m_e c^2$ , as consistent with the non adiabatic nature of the interaction between the laser pulse and the electrons.

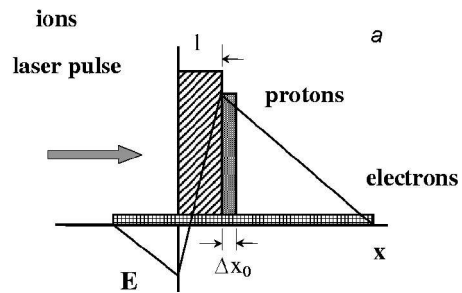


Рис. 1 а Бузиков и др.

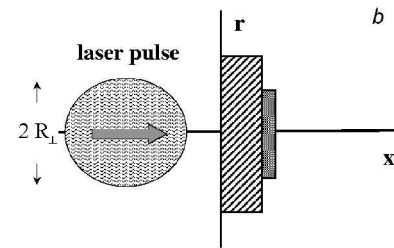


Рис. 1 б Бузиков и др.

Figure 4: Two-layer target. The rear side of the foil of heavy ions is coated with a thin hydrogen layer.

For  $a_0 \simeq 1$ , which corresponds for a  $\lambda \approx 1\mu m$  pulse wavelength to a laser intensity of the order of  $10^{18} \text{ Watt/cm}^2$ , the electrons can reach energies up to several *Mev*, while the energy of the fast ions can be as high as  $\sim 1 \text{ Gev}$ .

Although the 1-D approximation overestimate the energies achievable, these results indicate that with a proper optimization of the interaction conditions, one can achieve high proton energies even with modest laser pulse intensities.

These analytical considerations are supported by detailed numerical simulations<sup>14</sup> and recent experimental results<sup>15</sup>. See also discussion in<sup>16</sup>

---

<sup>14</sup>S. Bulanov *et al.*, *Plasma Phys. Rep.* , **28**, 453 (2002); S. Bulanov *et al.*, *Phys. Lett. A* **299**, 240 (2002); S.V. Bulanov, *et al.*, *Plasma Phys. Reports*, 30, 196 (2004).

<sup>15</sup>H. Schworer, *et al.*, *Nature*, bf 439, 445 (2006)

<sup>16</sup>B. J. Albright, *et al.*, *Phys. Rev. Lett.* **445**, 115002 (2006)

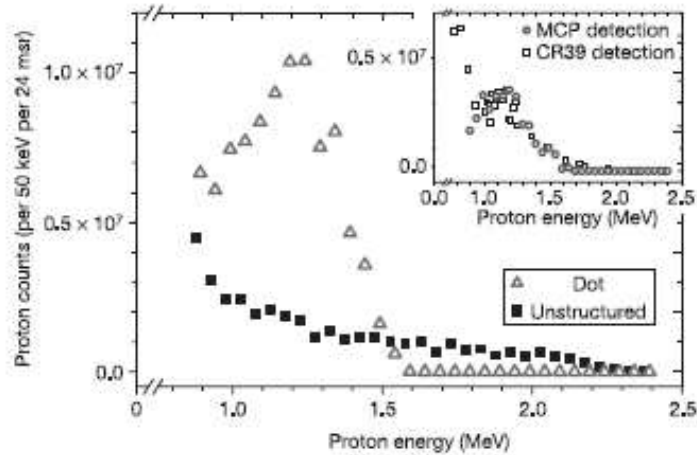


**Figure 3 | Proton spectra from the Thomson spectrometer.** The proton number reaching the detector is given per energy interval of 0.05 MeV and per solid angle of 24 msr versus proton energy. The main graph shows a spectrum obtained from irradiating the foil at the position of a dot using the MCP detection. It is represented by blue triangles. The spectrum from a dot exhibits a peak at an energy of 1.2 MeV as opposed to exponential spectra (black squares, average from six shots) in the case of using an unstructured part of the target foil. The peaked structure contains about  $10^8$  protons per 24 msr. The inset shows the comparison of the two detection systems: both spectra show the energy distribution of the protons from irradiating a dot under the same conditions. Red circles represent MCP detection, while black squares originate from CR39 detection.

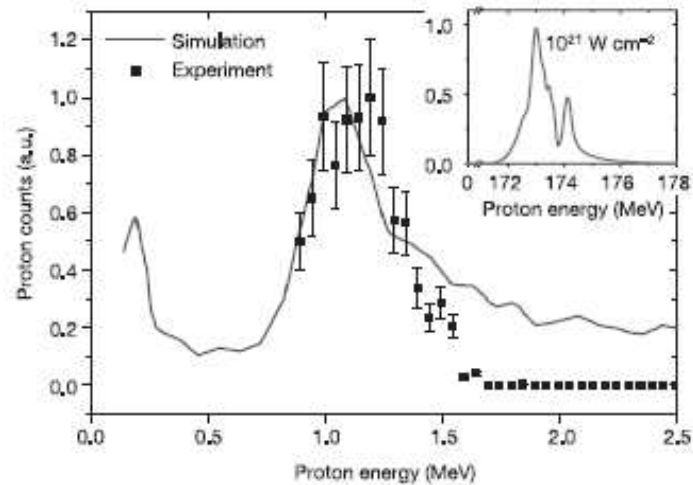


**Figure 4 | Results from simulations and scalability of the technique.** Comparison of experimental data (black squares) to the proton spectrum obtained from two-dimensional-PIC simulation (red line) for following conditions: laser intensity  $I_L = 3 \times 10^{19} \text{ W cm}^{-2}$ , and target dimensions  $5 \mu\text{m Ti foil} + 0.5 \mu\text{m PMMA dot } (20 \times 20) \mu\text{m}^2$ . Experimental data points comprise the observable energy range on the MCP detector. The statistical uncertainty for the measured data has a value of 20% s.d. as shown by the error bars. In the inset a simulation for a petawatt-laser system demonstrating the scalability of proton acceleration from microstructured targets is shown. The parameters for the simulation are  $I_L = 1.2 \times 10^{21} \text{ W cm}^{-2}$ ,  $5 \mu\text{m Ti foil} + 0.1 \mu\text{m PMMA dot } (2.5 \mu\text{m diameter})$ . The proton spectrum exhibits a narrow peak with relative energy width of  $\Delta E/E \approx 1\%$  at a peak energy of 173 MeV.

## High efficiency acceleration regimes

A regime of ion acceleration that exhibits very favourable properties has been recently identified along these lines<sup>17</sup>

In this regime the radiation pressure of the electromagnetic wave plays a dominant role in the interaction of an ultraintense laser pulse with a foil.

---

<sup>17</sup>T. Zh. Esirkepov, *et al.*, *Phys. Rev. Lett.* , **92** (2004) 175003.  
S. V. Bulanov, *et al.*, *Plasma Phys. Rep.*, **30** (2004) 196.

Radiation pressure can be a very effective mechanism of momentum transfer to charged particles.

This mechanism was introduced long ago<sup>18</sup>.

Physical conditions of interest range from stellar structures and radiation generated winds<sup>19</sup>, to high accuracy optical experiments<sup>20</sup> and optical traps, to the formation of “photon bubbles” in very hot stars and accretion disks<sup>21</sup>.

---

<sup>18</sup>A.S. Eddington, *MNRAS* **85**, 408 (1925).

<sup>19</sup>E.A. Milne, *MNRAS* **86**, 459 (1926); S. Chandrasekhar, *MNRAS* **94**, 522 (1934), N.J. Shaviv, *ApJ* **532**, L137 (2000).

<sup>20</sup>P.F. Cohadon, *et al.*, *Phys. Rev. Lett.* **83**, 3174 (1999), A. Ashkin, *Phys. Rev. Lett.* **24**, 156 (1970).

<sup>21</sup>J. Arons, *ApJ* **388**, 561 (1992); C.F. Gammie, *MNRAS* **297**, 929 (1998); M.C. Begelman, *ApJ* **551**, 897 (2001).

Particle acceleration by radiation pressure has been considered in the laboratory<sup>22</sup> and in high energy astrophysical environments<sup>23</sup>.

Radiation pressure arises from the “coherent” interaction of the radiation with the particles in the medium.

---

<sup>22</sup>T. Esirkepov, *et al.*, *Phys. Rev. Lett.* **92**, 175003 (2004); S.V. Bulanov, *et al.*, *Plasma Phys. Rep.* **30**, 196 (2004); F. Pegoraro, *et al.*, *Phys. Lett. A* **347**, 133 (2005); W. Yu, *et al.*, *Phys. Rev. E* **72**, 046401 (2005), A. Macchi, *et al.*, *Phys. Rev. Lett.* **94**, 165003, (2005); J. Badziak, *et al.*, *Appl. Phys. Lett.* **89**, 061504, (2006).

<sup>23</sup>P. Goldreich, *Phys. Scripta* **17**, 225 (1978); T. Piran, *ApJ* **257**, L23 (1982); V. S. Berezinskii, *et al.*, *Astrophysics of Cosmic Rays*, (Elsevier, Amsterdam, 1990).

In an electron-ion plasma, radiation pressure acts mostly on the lighter particles, the electrons, with a force that is quadratic in the wave field amplitude.

Ions on the contrary are accelerated by the charge separation field caused by the electrons pushed by the radiation pressure.

This collective acceleration mechanism is very efficient<sup>24</sup> when the number of ions inside the electron cloud is much smaller than that of the electrons.

---

<sup>24</sup>V.I. Veksler, in *Proc. CERN Symposium on High Energy Accelerators and Pion Physics*, Geneva, **1**, 80 (1956).

## The RPDA Regime

As already mentioned, different regimes of plasma ion acceleration have been discussed in the literature<sup>25</sup>

A critical factor for a number of applications is the efficiency of the energy conversion.

In the Radiation Pressure Dominant Acceleration (RPDA) the ion acceleration in a plasma is directly due to the radiation pressure of the e.m. pulse<sup>26</sup>.

---

<sup>25</sup>S.V. Bulanov, *et al.*, in *Reviews of Plasma Physics*, ed. V.D. Shafranov, **22**, 227 (Kluwer Acad., N.Y., 2001); G.A. Mourou, *et al.*, *Rev. Mod. Phys.* **78**, 309 (2006) + references therein.

<sup>26</sup>T. Esirkepov, *et al.*, *Phys. Rev. Lett.* **92**, 175003 (2004); S.V. Bulanov, *et al.*, *Plasma Phys. Rep.* **30**, 196 (2004).

In this regime, the ions move forward with almost the same velocity as the electrons and thus have a kinetic energy well above that of the electrons.

This acceleration process is highly efficient and the ion energy per nucleon is proportional to the e.m. pulse energy.

*This acceleration mechanism can be illustrated by considering a thin, dense plasma foil, made of electrons and protons, pushed by an ultra intense laser pulse in conditions where the radiation cannot propagate through the foil, while the electron and the proton layers move together and can be regarded as forming a (perfectly reflecting) relativistic plasma mirror co-propagating with the laser pulse.*

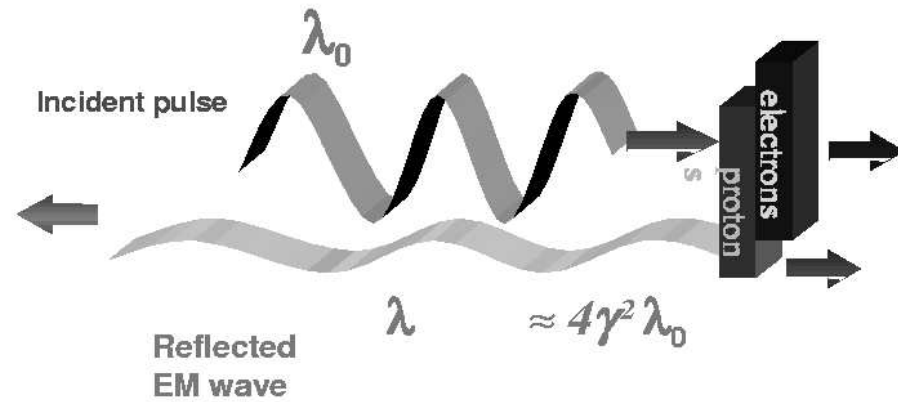


Figure 7: Mirror reflection

The frequency of the reflected e.m. wave is reduced by

$$\frac{(1 - v/c)}{(1 + v/c)} \approx \frac{1}{4}\gamma^2, \quad \text{with } \gamma = (1 - v^2/c^2)^{-1/2}$$

and  $v$  the mirror velocity.

Thus the plasma mirror is accelerated and acquires from the laser the energy

$$(1 - 1/4\gamma^2)\mathcal{E},$$

where  $\mathcal{E}$  is the incident laser pulse energy in the laboratory frame (LF).

For large values of  $\gamma$  practically all the e.m. pulse energy is transferred to the mirror, essentially in the form of proton kinetic energy.

This high efficiency of the e.m. energy conversion into the fast protons opens up a wide range of applications.

For example it can be exploited in the design of proton dump facilities for spallation sources or for the production of large fluxes of neutrinos<sup>27</sup>.

---

<sup>27</sup>S.V. Bulanov, *et al.*, *Nucl. Instr. Meth. A* **540**, 25 (2005).

## Rayleigh-Taylor instabilities

*Both in the astrophysical and in the laser plasma contexts, the onset of Rayleigh-Taylor-like instabilities<sup>28</sup> may affect the interaction of the plasma with the radiation pressure.*

In this case the e.m. radiation may eventually dig through the plasma and make it porous to the radiation (and allow e.g., for super-Eddington luminosities) or, in the case of a plasma foil accelerated by a laser pulse, may tear it into clumps<sup>29</sup> and broaden the energy spectrum of the fast ions.

---

<sup>28</sup>Heavier medium accelerated by a lighter medium.

<sup>29</sup>K. Kifonidis, *et al.*, *Astron. Astrophys.* **408**, 621 (2003).

In this last part I will discuss the stability of a plasma foil in the ultra relativistic conditions that are of interest for the RPDA regime<sup>30</sup>.

We find that

- in the relativistic regime the growth of the instability is slower than in the nonrelativistic regime
- proper tailoring of the pulse amplitude can allow for stable foil acceleration.
- With the help of two-dimensional (2D) Particle in cell (PIC) simulations, we find that the nonlinear development of the instability leads to the formation of *high-density, high-energy plasma clumps*.

---

<sup>30</sup>Photon bubbles and ion acceleration in a plasma dominated by the radiation pressure of an electromagnetic pulse, F. Pegoraro, S.V. Bulanov, (2007) submitted to Phys. Rev. Lett.

## Radiation Pressure Acceleration of a thin foil Mirror

The equation of motion of an element of area  $|d\sigma|$  of a perfectly reflecting mirror can be written in the LF as

$$d\mathbf{p}/dt = Pd\sigma,$$

where  $\mathbf{p}$  is the momentum of the mirror element,  $d\sigma$  is normal to the mirror surface and  $P$  is the Lorentz invariant radiation pressure.

For the sake of geometrical simplicity, we refer to a 2D configuration where the mirror velocity and the mirror normal vector remain coplanar (in the  $x$ - $y$  plane,  $x$  being the direction of propagation of the e.m. pulse), i.e., we assume that the mirror does not move or bend along  $z$ .

The radiation pressure  $P$  is given in terms of the amplitude of the electric field  $E_M$  of the incident e.m. pulse and of the pulse incidence angle  $\theta_M$  in the CMF by

$$P = (E_M^2/2\pi) \cos^2 \theta_M,$$

where

$$E_M^2 = (\omega_M^2/\omega_0^2) E_0^2$$

with

$$\omega_M^2/\omega_0^2 = (1 - \beta \cos \phi)^2/(1 - \beta^2),$$

the subscript 0 denotes quantities in the LF and  $\phi$  the angle the mirror velocity  $\beta$  makes with the  $x$ -axis in the laboratory frame. The angle  $\theta_M$  vanishes when the incidence angle  $\theta_0$  in the LF vanishes and  $\phi = 0, \pi$ , but is a fast increasing function of  $\gamma$  for  $\theta_0 \neq 0$ , or  $\phi \neq 0, \pi$ <sup>31</sup>.

---

<sup>31</sup>Kinematic considerations show that the laser pulse can no longer reach the receding mirror when  $|\sin \phi| > 1/\gamma$ . This inequality constrains the maximum value of  $\gamma$  that can be obtained with a non perfectly collimated beam, see also E.S. Phinney, *MNRAS* **198**, 1109 (1982).

Then, the equation of motion of a mirror element of unit length along  $z$  and uniform density  $n_0$  in the LF is

$$\bullet \bullet \quad \frac{\partial p_x}{\partial t} = \frac{P}{n_0 l_0} \frac{\partial y}{\partial s}, \quad \frac{\partial p_y}{\partial t} = -\frac{P}{n_0 l_0} \frac{\partial x}{\partial s} \quad (1)$$

with

$$\frac{\partial x}{\partial t} = \beta_x c \quad \text{and} \quad \frac{\partial y}{\partial t} = \beta_y c.$$

Here

$$p_{x,y} = m_i c \frac{\beta_{x,y}}{(1 - \beta^2)^{1/2}}$$

are the spatial components of the momentum 4-vector of the mirror element,  $l_0$  is the mirror thickness and  $m_i$  is the ion mass.

Lagrangian coordinates,  $x_0$  and  $y_0$ , have been adopted such that  $x, y = x, y(x_0, y_0, t)$  and  $ds = (dx_0^2 + dy_0^2)^{1/2}$ .

In the non relativistic limit and for constant  $P$ , Eqs.(1) coincide with Ott's equations<sup>32</sup> for the motion of a thin foil.

Assuming that the unperturbed mirror moves along the  $x$ -axis, i.e. that the initial conditions correspond to a flat mirror along  $y_0$ , so that  $dx_0 = 0$ ,  $dy_0 = ds$  and  $\theta_M = 0$ , we write Eqs.(1) as<sup>33</sup>

$$\frac{dp_x^0}{dt} = \frac{E_0^2}{2\pi n_0 l_0} \frac{m_i c \gamma_0 - p_x^0}{m_i c \gamma_0 + p_x^0}, \quad (2)$$

where  $p_x^0$  is the unperturbed  $x$  component of momentum and depends on the variable  $t$  only and  $m_i^2 c^2 \gamma_0^2 = m_i^2 c^2 + (p_x^0)^2$ .

---

<sup>32</sup>E. Ott, *Phys. Rev. Lett.* **29**, 1429 (1972).

<sup>33</sup>Eq.(2) has been analyzed in T. Esirkepov, *et al.*, *Phys. Rev. Lett.* **92**, 175003 (2004) and S.V. Bulanov, *et al.*, *Plasma Phys. Rep.* **30**, 196 (2004)

The electric field of the e.m. pulse at the mirror position  $x(t)$  depends on time as  $E_0 = E_0[t - x(t)/c]$ .

Let us introduce the phase of the wave  $\psi = \omega_0[t - x^0(t)/c]$ , at the unperturbed mirror position  $x^0(t)$  as a new independent variable. Differentiating with respect to time, we obtain

$$\frac{d\psi}{dt} = \omega_0 \frac{m_i c \gamma_0 - p_x^0}{m_i c \gamma_0}. \quad (3)$$

Using the variable  $\psi$  and the normalized fluence of the e.m. pulse

$$w(\psi) = \int_0^\psi (R(\psi')/\lambda_0) d\psi',$$

with

$$R(\psi) = E_0^2(\psi)/(m_i n_0 l_0 \omega_0^2),$$

and  $\lambda_0 = 2\pi c/\omega_0$ , the solution of Eq.(2) with the initial condition  $p_x^0(0) = 0$  is

$$\bullet \bullet \quad p_x^0(\psi) = m_i c \frac{w(\psi)[w(\psi) + 2]}{2[w(\psi) + 1]}, \quad (4)$$

while from Eq.(3) we obtain that  $t$  and  $\psi$  are related by

$$\bullet \bullet \quad \psi + \int_0^\psi [w(\psi') + w^2(\psi')/2] d\psi' = \omega_0 t. \quad (5)$$

For a constant amplitude e.m. pulse, when  $R = R_0$ , these expressions reduce to

$$w(\psi) = (R_0/\lambda_0) \psi$$

, and to

$$\psi + (R_0/\lambda_0) \psi^2/2 + (R_0/\lambda_0)^2 \psi^3/6 = \omega_0 t, \quad (6)$$

with

$$p_x^0 \approx m_i c (R_0/\lambda_0) \omega_0 t$$

for  $t \ll \omega_0^{-1} (\lambda_0/R_0)$  and, for  $t \gg \omega_0^{-1} (\lambda_0/R_0)$ ,

$$\bullet \bullet \quad p_x^0 \approx m_i c (3R_0 \omega_0 t / 2\lambda_0)^{1/3} .$$

These relationships are obtained under the assumption that the charge separation electric field  $E_{||}$  which accelerates the ions is sufficiently large, so that

$$E_{||} = 2\pi n_0 e l_0 > (E_0^2 / 2\pi n_0 l_0) [(m_i c \gamma_0 - p_x^0) / (m_i c \gamma_0 + p_x^0)] .$$

The latter condition can be rewritten in terms of the dimensionless laser pulse amplitude

$$a_0 = eE_0/m_e\omega_0$$

and of the dimensionless parameter<sup>34</sup>

$$\epsilon_0 = 2\pi n_0 e^2 l_0 / m_e \omega_0 c \quad \text{as}$$

$$a_0 < \epsilon_0 [(m_i c \gamma_0 + p_x^0 / m_i c \gamma_0 - p_x^0)^2]^{1/2}$$

and is equivalent to the full opacity condition for a thin overdense plasma foil in the CMF. In the opposite limit the ions are accelerated by the electric field

$$E_{||} = 2\pi n_0 e l_0 \quad \text{until} \quad p_x^0 m_i c (2a_0 / \epsilon_0)^{1/2}$$

when they enter the RPDA regime.

<sup>34</sup>V.A. Vshivkov, *et al.*, *Phys. Plasmas* **5**, 2727 (1998).

## The Instability of the accelerated foil

Let us now investigate the linear stability of the accelerated mirror with respect to perturbations  $x^1(y_0, \psi)$ ,  $y^1(y_0, \psi)$  that bend the plasma foil. Linearizing Eqs.(1) around the solution given by Eq.(4) we obtain

$$\bullet \bullet \quad \frac{\partial}{\partial \psi} \left[ \frac{p_x^0(\psi)}{m_i c} \frac{\partial x^1}{\partial \psi} \right] = \frac{R(\psi)}{2\pi} \frac{\partial y^1}{\partial y_0}, \quad (7)$$

$$\bullet \bullet \quad \frac{\partial}{\partial \psi} \left[ \frac{m_i c}{p_x^0(\psi)} \frac{\partial y^1}{\partial \psi} \right] = -\frac{R(\psi)}{2\pi} \frac{\partial x^1}{\partial y_0}. \quad (8)$$

Here we retain only the leading terms in the ultrarelativistic limit  $p_x^0/m_i c \gg 1$  for the foil motion and neglect a term proportional to  $(\partial R/\partial \psi) x^1/\lambda_0$ .

We look for WKB solutions of the form

$$y^1(y_0, \psi) \propto \exp \left[ \int_0^\psi \Gamma(\psi') d\psi' - iky_0 \right], \quad (9)$$

with growth rate  $\Gamma \gg 1$ . We find

$$\Gamma(\psi) = [kR(\psi)/2\pi]^{1/2}, \quad \text{with} \quad x^1 \sim -iy^1(m_i c/p_x^0).$$

For a constant amplitude pulse, using Eq.(6), we obtain

$$y^1 \propto \exp \left[ (t/\tau_r)^{1/3} - iky_0 \right], \quad (10)$$

where

$$\bullet \bullet \quad \tau_r = \omega_0^{-1} (2\pi)^{3/2} R_0^{1/2} / (6k^{3/2} \lambda_0^2)$$

is the characteristic time of the instability in the ultrarelativistic limit.

**The time scale of the instability is proportional to the square root of the ratio between the the radiation pressure and the ion mass.**

*Thus, the larger the ion mass, the faster the perturbation grows while the larger the radiation pressure the slower the perturbation.*

In the non-relativistic limit the perturbation grows as

$$x^1, y^1 \propto \exp [t/\tau - ik y_0], \quad (11)$$

where

$$\tau = \omega_0^{-1} (2\pi/kR_0)^{1/2},$$

In the ultrarelativistic limit the instability develops more slowly with time than in the non-relativistic case:  $t^{1/3}$  instead of  $t$ . In addition the nonrelativistic time  $\tau$  is inversely proportional to the square root of the radiation pressure.

If we express Eqs.(10,11) in terms of the unperturbed momentum  $p_x^0$ , in both limits we find an exponential growth of the form

$$\bullet \bullet \quad y^1(y_0, p_x^0) \propto \exp \left[ \kappa p_x^0 / (m_i c) - i k y_0 \right],$$

where

$$\kappa = (k \lambda_0)^{1/2} / (2\pi R_0 / \lambda_0)^{1/2}$$

i.e.,

$$\kappa \propto (k/l_0)^{1/2} (m_i/m_e)^{1/2} (\omega_{pe,0}/\omega_0) a_0^{-1},$$

with

$$\omega_{pe,0}^2 = 4\pi n_0 e^2 / m_e.$$

## Stabilization with tailored EM pulses

This exponential growth of the perturbation with the unperturbed momentum for a constant amplitude pulse can be stopped by tailoring the shape of the e.m. pulse. We refer to the ultrarelativistic limit and define  $\Phi(\psi) = \int_0^\psi \Gamma(\psi') d\psi'$ . From Eq.(4), which in this limit takes the form

$$p_x^0(\psi) = m_i c \int_0^\psi (R(\psi')/2\lambda_0) d\psi',$$

we see that the stability condition can be formulated as follows: *it is possible to choose the dependence of the e.m. pressure  $R(\psi)$  on the phase  $\psi$  such that, for  $\psi \rightarrow \psi_m$ , the ion momentum  $p_x^0(\psi)$  grows, formally to infinity, while  $\Phi(\psi)$  remains finite. Here  $\psi_m$  is either finite or equal to infinity.*

As an example we can take  $R(\psi)$  of the form

$$R(\psi) = R_0(1 - \psi/\psi_m)^{-\alpha} \chi(\psi_1 - \psi),$$

with  $1 < \alpha < 2$ ,  $\chi(x) = 1$  for  $x > 0$ , and  $\chi(x) = 0$  for  $x < 0$  and  $\psi_m > \psi_1$  so as to keep the pulse fluence finite.

In this case the maximum value of the ion momentum

$$p_x^0/(m_i c) \approx R_0 \psi_m (1 - \psi_1/\psi_m)^{1-\alpha} / [2\lambda_0(\alpha - 1)],$$

tends to infinity for  $\psi_1 \rightarrow \psi_m$ , while

$$\Phi(\psi_m) = (2kR_0/\pi)^{1/2} \psi_m [1 - (1 - \psi_1/\psi_m)^{1-\alpha/2}] / (2 - \alpha)$$

remains finite. In addition, for  $\alpha < 3/2$  the acceleration time is finite.

## Results of PIC Simulations

The PIC simulations presented in T. Esirkepov, *et al.*, *Phys. Rev. Lett.* **92**, 175003 (2004); S.V. Bulanov, *et al.*, *Plasma Phys. Rep.* **30**, 196 (2004); show a stable phase of the RPDA of protons where a portion of the foil, with the size of the pulse focal spot, is pushed forward by a super-intense e.m. pulse.

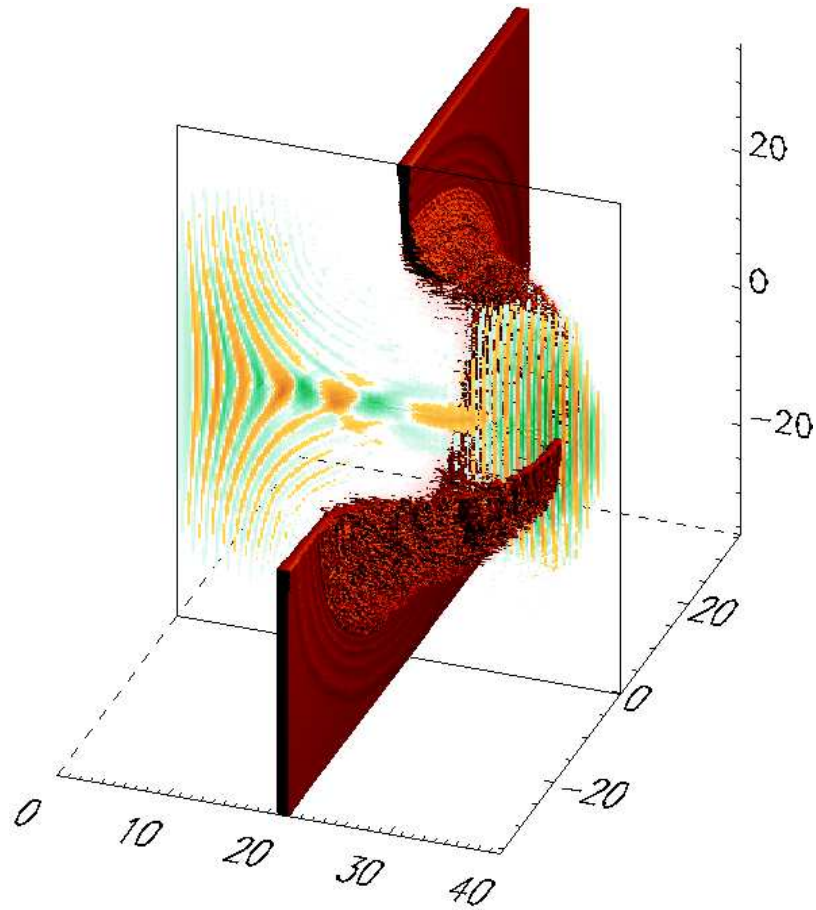


Figure 8: Radiation Pressure Acceleration of a thin foil

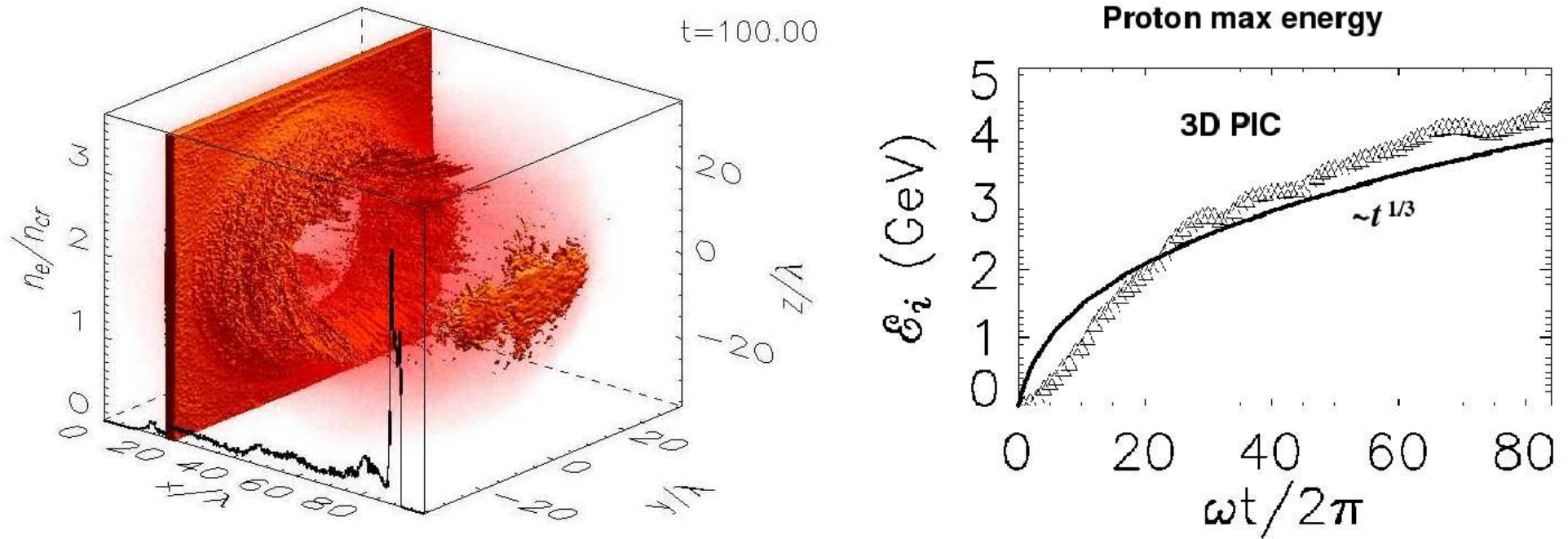


Figure 9: Ion acceleration

The wavelength of the reflected radiation is substantially larger than that of the incident pulse, as consistent with the light reflection from the co-moving relativistic mirror with the e.m. energy transformation into the kinetic energy of the plasma foil.

At this stage, the initially planar plasma slab is transformed into a “cocoon” inside which the laser pulse is almost confined. The protons at the front of the “cocoon” are accelerated up to energies in the multi-GeV range at a rate that agrees with the  $t^{1/3}$  scaling predicted by the analytical model. The proton energy spectrum has a narrow feature corresponding to a quasi-monoenergetic beam, but part of it extends over a larger energy interval.

In order to investigate the onset and the nonlinear evolution of the instability of the foil we have performed a series of numerical simulations with heavier ions (aiming at a faster growth rate), using the 2D version of the PIC e.m. relativistic code REMP, which is based on the “density decomposition” scheme<sup>35</sup>.

The size of the computation box is  $95\lambda \times 40\lambda$  with a mesh of 80 cells per  $\lambda$ . Such a high spatial resolution is required because the interaction of a super intense e.m. pulse with an overdense plasma slab is accompanied by strong plasma compression.

The total number of quasi-particles in the plasma region is equal to  $2 \times 10^6$ .

A thin plasma slab, of width  $20\lambda$  and thickness  $0.5\lambda$ , is localized at  $x = 20\lambda$ . The plasma is made of fully ionized aluminum ions with  $Z = 13$ , the ion to electron mass ratio is  $26.98 \times 1836$ . The electron density is equal to  $64n_{cr}$ , with  $n_{cr} = \omega_0^2 m_e / 4\pi e^2$  the critical density.

---

<sup>35</sup>T. Esirkepov, *Comput. Phys. Commun.* **135**, 144 (2001).

An  $s$ -polarized laser pulse with electric field along the  $z$ -axis is initialized in vacuum at the left-hand side of the plasma slab.

The pulse has a "gaussian" envelope given by  $a_0 \exp(-x^2/2l_x^2 - y^2/2l_y^2)$ , with  $l_x = 40\lambda$ ,  $l_y = 20\lambda$ .

The dimensionless pulse amplitude,  $a_0$ , corresponds for  $\lambda = 1\mu m$  to the intensity  $I = 1.37 \times 10^{23} \text{ W/cm}^2$ , close to the value that is expected for the recently proposed super-power lasers such as *HiPER* and *ELI*<sup>36</sup>.

The boundary conditions are periodic along the  $y$ -axis and absorbing along the  $x$ -axis for both the e.m. radiation and the quasi-particles.

For our choice of the laser-target parameters the opacity condition is fulfilled.

The results of these simulations are shown in the following figures at  $t = 75, 87.5$ .

---

<sup>36</sup>M. Dunne, *Nature Physics* **2**, 2 (2006); M. Schirber, *Science* **310**, 1610 (2005); <http://www.hiper-laser.org/>; <http://loa.ensta.fr/> .

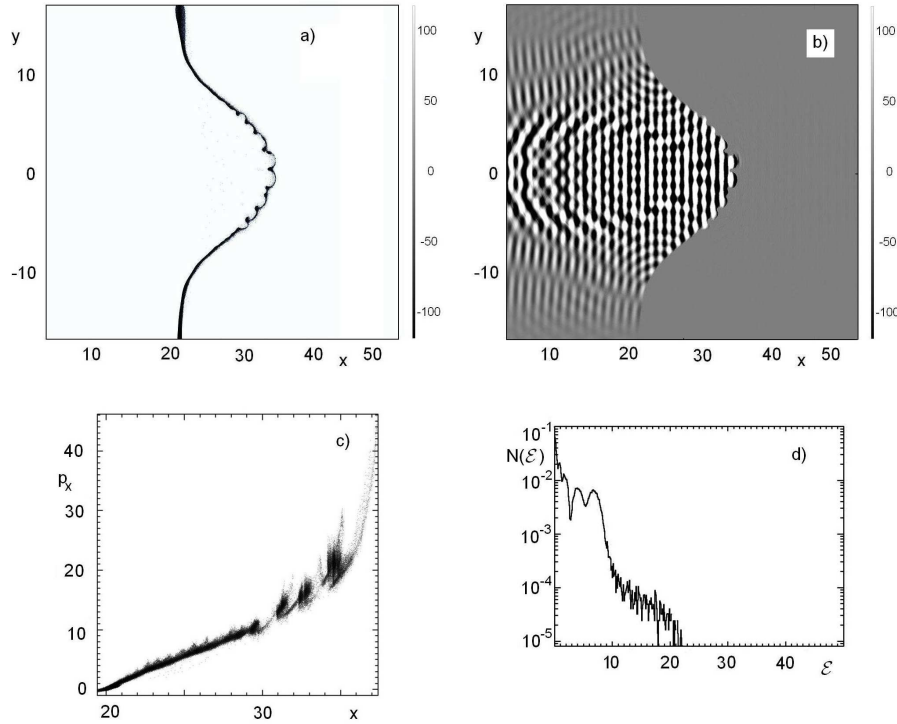


Figure 10: a): ion density distribution in the  $x$ - $y$  plane; b) distribution of the electric field  $E_z$ ; c) ion phase plane ( $p_x$ ,  $x$ ); d) ion energy spectrum at  $t = 75$ .

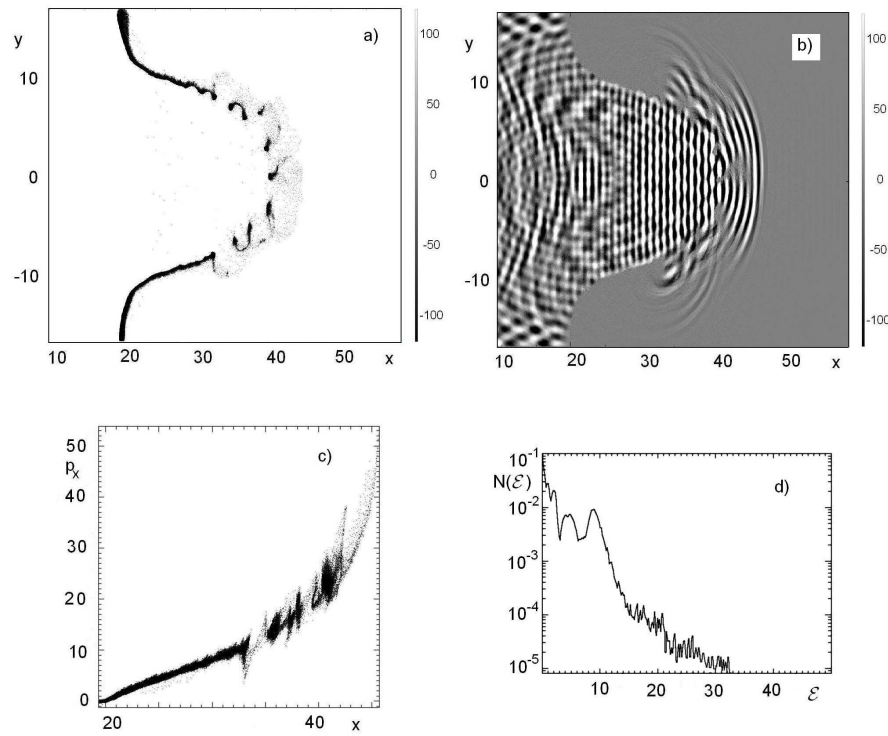


Figure 11: Same as in Fig.1 but at  $t = 87.5$ .

The distribution in the  $x$ - $y$  plane of the ion density and of the  $z$ -component of the electric field  $E_z$  are shown in frames a) and b), frames c) show the ion phase plane,  $(p_x, x)$  and frames d) the energy spectrum of the aluminum ions. The ion momentum and kinetic energy are given in GeV/ $c$  and in GeV, respectively. The wavelength  $\lambda$  of the incident radiation and its period  $2\pi/\omega_0$  are chosen as units of length and time.

We see the typical initial stage of the Rayleigh-Taylor instability with the formation of cusps and of multiple-bubbles in the plasma density distribution. These are accompanied by a modulation of the e.m. pulse at its front,

At this time the ions are accelerated forward, as seen in their phase plane. Their energy spectrum is made up of quasi-monoenergetic beamlets which correspond to the cusp regions, and of a relatively high energy tail which is formed by the ions at the front of the bubbles.

At  $t = 87.5$  we see that the fully nonlinear stage of the instability results in the formation of several clumps in the ion density distribution with more diffuse, lower density plasma clouds between them.

The e.m. wave partially penetrates through, and partially is scattered by, the clump-plasma layer.

The high energy tail in the ion spectrum grows much faster than in the stable case.

At later times, because of the mass reduction of the diffuse clouds at the front of the pulse, the maximum ion energy scales linearly with time.

The local maxima at relatively lower energy correspond to the plasma clumps.

## Conclusions on the last part

In the relativistic regime the Rayleigh-Taylor instability of a plasma foil accelerated by the radiation pressure of the reflected e.m. pulse develops much more slowly than in the non-relativistic regime.

In the former limit its timescale is inversely proportional to the square root of the ratio between the radiation pressure and the ion mass while in the latter this dependence is reversed.

The use of a properly tailored e.m. pulse with a steep intensity rise can stabilize the shell acceleration.

Numerical simulations show that the nonlinear development of the instability leads to the formation of high-density, high-energy plasma clumps and to a relatively higher rate of ion acceleration in the regions between the clumps.

For the HiPER and ELI laser systems the ion energy can easily reach several tens of GeV.